CHAPTER VII
BIOCOMPATIBLE EVALUATION IN VITRO OF POLY(ε-CAPROLACTONE)/POLY(3-HYDROXYBUTYRATE-*CO*-3-HYDROXYVALERATE) FIBROUS SUBSTRATES FILLED WITH PROTEIN-LOADED HYDROXYAPATITE PARTICLES

7.1 Abstract

To improve both osteoconductive and osteoinductive properties of the polymeric substrate, hydroxyapatite (HAp) (1% w/v based on the volume of the base 10 wt% of 50/50 w/w PCL/PHBV solution in 80/20 v/v chloroform/dimethylformamide) loaded with three different proteins, e.g. crude bone protein (CBP), fibronectin (FN) and type-I collagen (COL) (HAp/proteins), was incorporated into electrospun fibrous matrices of poly(ε-caprolactone) (PCL)/ poly(3-hydroxybutyrate-*co*-3-hydroxyvalerate) (PHBV). Even though the presence of HAp and HAp/proteins made the morphology of the individual fibers slightly less uniform, there were no significant differences of the hydrophilicity and mechanical integrity among the fibrous matrices. The potential use of these fibrous matrices as bone substrates was assessed by mouse calvaria-derived pre-osteoblastic cells, MC3T3-E1, in terms of attachment, proliferation, differentiation, and mineralization. The three types of proteins showed the differences in their loaded and released amounts, which considerably affected the cell differentiation and mineralization. Due to the highest release amount of CBP from the PCL/PHBV-HAp/CBP fibrous substrate, MC3T3-E1 cultured on the surface of the PCL/PHBV-HAp/CBP fibrous substrate expressed the greatest amount of alkaline phosphatase (ALP) activity on day 7 and mineralization on day 14 after cell culturing. The obtained results suggested that the PCL/PHBV-HAp/CBP fibrous substrate has a high potential to be used as a synthetic bone substitute for bone regeneration.

(**Key-words**: PCL; PHBV; Hydroxyapatite; Crude bone protein; Fibronectin; Collagen)

7.2 Introduction

Development of materials for bone reconstruction applications has been highly influenced by the advent of tissue engineering. Biomaterials are developed especially on tissue regeneration to promote specific cellular responses (Hench *et al.*, 2002). New tissues are generated through the combination of synthetic scaffolds, cells, and active substances such as morphogenetic proteins and growth factors (Ito, 1998; Hutmacher, 2000). With many advantages such as accelerating the growth of the surrounding tissues, improving biological properties, and enhancing therapeutic efficacy, electrospun fibrous scaffolds have been explored as new devices for dental repair (Deng *et al.*, 2007), ligament reconstruction (Vaquette *et al.*, 2010), and protein/drug delivery system (Chew, 2005; Kenawy, 2009).

For fabricating the electrospun fibrous scaffolds, synthetic biodegradable polyester such as poly(lactic acid) (PLA), poly(glycolic acid) (PGA), poly(ε-caprolactone) (PCL) and poly(3-hydroxybutyrate-*co*-3-hydroxyvalerate) (PHBV) are the preferred choices owing to their good processability, biocompatibility, and mechanical performance. Obviously, these synthetic polymers have replicated the physical dimensions and morphology of the major component (collagen) in the native extracellular matrix (ECM) as biologically (Boland, 2006; Sangsanoh, 2007; Hubbell, 1995). Merely a kind of synthetic polymer, however, might not reach optimal conditions of biological, physical, and mechanical properties for the use in the engineering of a variety of tissue. Therefore, hybridizing synthetic polymers, polymer blends or polymer composites were developed.

The fibrous scaffold of the poly(3-hydroxybutyrate-*co*-3-hydroxyvalerate)/poly(L-lactic acid) (PHBV/PLLA) blend appeared to yield the best results regarding cell number increase, their attachment, and spreading inside and on the scaffold compared to the pure ones (Ndreu *et al.*, 2008). A poly(ε-caprolactone)/ poly(3-hydroxybutyrate-*co*-3-hydroxyvalerate) (PCL/PHBV) blend was reported having superior mechanical properties in terms of tensile modulus and tensile strength compared to pure PCL (Del *et al.*, 2011). Physically, this blend also provided both better hydrophilicity (wettability) and greater biodegradability. Biologically, this blend could higher promote cell-surface recognition and control

cell physiology such as adhesion, spreading, activation, proliferation, differentiation, and mineralization (K-hasuwan, 2011; Gonçalves, 2010) than the pure PCL and PHBV.

Apart from the blends of polymers, the nanoparticles have been incorporated into polymers as polymer composites to add functionalities and/or to improve mechanical properties particularly for bone tissue engineering. Synthetic hydroxyapatite (HAp), one of bioactive calcium phosphate based ceramic nanoparticles, has been employed extensively as implant material for bone substitute due to its good osteoconductivity (Rameshbabu *et al.*, 2005). The HAp nanoparticles have excellent properties to increase surface area and enhance the ability of controlled release of chemical species for promoting cell response and proliferation to induce mineralization in bone tissue engineering (Yuan, 1998; Akao, 1993). The HAp nanoparticles in the composite played a critical role in the process of implant osteointegration, as the polymer matrix degraded. New bone formation at the implant interface was observed for the study of PHBV-HAp composite *in vivo*, indicating a potential use of the PHBV-HAp composite to guide bone reconstruction (Luklinska *et al.*, 2003). Similar results were reported for composite scaffolds of PCL-HAp, which could support osteogenic differentiation of mouse calvaria-derived pre-osteoblastic cells (MC3T3-E1) (Wutticharconmongkol *et al.*, 2007) and human primary bone cells (Chuenjitkuntaworn *et al.*, 2010).

Incorporating cell-signaling molecules such as peptides and growth factors have been proven to further improve the cellular behavior of the tissue engineering scaffolds. A significant increased mineralization (55%) in PCL/HAp/Collagen biocomposite nanofibrous scaffolds of cell culture using human fetal osteoblast cells (hFOB), suggesting that the biocomposite scaffolds had inherent surface functionality for hFOB adhesion, migration, proliferation, and mineralization to form a bone tissue, was reported (Venugopal *et al.*, 2007). Correspondingly, PLLA/HAp and PLLA/Collagen/HAp nanofibers were fabricated by electrospinning. The results showed that the biocomposite PLLA/Collagen/HAp nanofibers appeared to be superior to PLLA/HAp nanofibers for bone regeneration (Prabhakaran *et al.*, 2009).

In the present contribution, PCL/PHBV fibrous substrates incorporating HAp loaded with three different proteins (HAp/proteins) were focused on. Crude

bone protein (CBP), fibronectin (FN), type-I collagen (COL) were selected as model proteins. The morphology, mechanical integrity, and physico-chemical properties of the composite PCL/PHBV-HAp/proteins fibrous substrates were investigated. The release kinetics and cell physiological effectiveness were also studied. The potential use of these composite fibrous substrates as bone regenerative materials was assessed *in vitro* in terms of the ability to support the attachment, proliferation, differentiation, and mineralization of the mouse calvaria-derived pre-osteoblastic cells, MC3T3-E1.

7.3 Experimental

7.3.1 Materials

Chemical reagents used in synthesizing the HAp including calcium hydrogen phosphate dihydrate ($CaHPO_4.2H_2O$, A.R. grade, Fluka), calcium carbonate ($CaCO_3$, A.R. grade, Carlo Erba), nitric acid (HNO_3, A.R. grade, Labscan), and tris (hydroxymethyl)-aminomethane (tris-base, A.R. grade, Sigma) were used without further purification. Model proteins used for generating HAp/protein composites were type-I collagen (COL) and fibronectin (FN) purchased from Sigma-Aldrich, USA, as well as crude bone protein (CBP) prepared from the pork bone Biodegradable polymers used in fabricating the fibrous scaffolds were poly(ε-caprolactone) (PCL; M_w = 80000 g mol^{-1}) and poly(3-hydroxybutyrate- *co*-3-hydroxyvalerate) (PHBV; M_w = 680 000 g mol^{-1}) purchased from Sigma-Aldrich, USA. *N,N*-dimethylformamide (DMF) and chloroform were used as the solvent purchased from Labscan (Asia), Thailand.

7.3.2 Preparation of Crude Bone Protein

Crude bone protein (CBP) was extracted from the pork bone by washing, cleansing, and sectioning the bone into small pieces. The small bone fragments were further crushed into powder in liquid nitrogen. Later, the as-prepared powder was immersed in 0.6 M HCL at 4 °C for 3 days. The solution was then centrifuged and the supernatant was collected, dialyzed, and lyophilized for 48 h. The obtained CBP was kept in the desiccators until use.

7.3.3 Synthesis of Hydroxyapatite/Protein Composites

Calcium carbonate ($CaCO_3$) and calcium hydrogen phosphate dihydrate ($CaHPO_4.2H_2O$) were used as precursors of calcium (Ca) and phosphorus (P) to prepare protein-encapsulated hydroxyapatite composites by fixing the molar ratios of Ca to P to be at 1.67. Briefly, 0.08 g of $CaCO_3$ and 0.2 g of $CaHPO_4.H_2O$ were dissolved in 1 M HNO_3 2.5 ml under stirring at 70 °C for 2 h and the pH of the solution was kept to 2. Type-I collagen (COL), fibronectin (FN), and crude bone protein (CBP) were added in the amount of 1 mg/ 50 ml of the mixed solution at room temperature. 20 ml of 1 M tris-base solution were then poured into the mixture generating the precipitation at pH 7. The precursor solution was stirred vigorously to yield a homogeneous product. The product was then filtered off and washed several times with deionized water. After centrifugation, the resulting material was freeze-dried for 48 h to obtain the fine powder products.

7.3.4 Preparation of Fibrous Substrates

Electrospun PCL/PHBV, PCL/PHBV-HAp, and PCL/PHBV-HAp/proteins fibrous substrates were prepared by electrospinning from 10 wt% of 50/50 w/w PCL/PHBV in 80/20 v/v chloroform/DMF or the same solution that contained 1% w/v HAp or HAp/proteins powder at room temperature. The as-prepared PCL/PHBV solution, the as-prepared PCL/PHBV-HAp suspension, or the as-prepared PCL/PHBV-HAp/proteins suspension was contained in a glass syringe, the open end of which connected to a blunt gauge-20 stainless steel hypodermic needle (o.d. = 0.91 mm) used as the nozzle. An Al sheet wrapped around a rotating cylinder (width and o.d. of the cylinder ~15 cm; rotational speed ~50 rpm) was used as a collector. The distance from the tip of the needle surface of the Al sheet defining the collection distance was fixed at 10 cm. A gamma high-voltage research D-ES30PN/M692 power supply was used to generate a high dc potential (i.e., 21 kV). The emitting electrode of positive polarity was connected to the needle, while the grounding one was connected to the collector. The feed rate of the solution/suspension was controlled at ~1 $mL \cdot h^{-1}$ by mean of a Kd Scientific syringe pump. The as-prepared solution/suspension was carried out continuously for ~10 h.

The thickness of the obtained PCL/PHBV, PCL/PHBV-HAp, and PCL/PHBV-HAp/proteins fibrous substrates was ~110 μm.

7.3.5 Characterization

The viscosities of the polymer solution/suspension were measured by a Brookfield DVIII Ultra rheometer at room temperature and 20 rpm rotational speed of the spindle ($n = 5$).

The morphological appearance and size of the individual fibers as well as those of the beads of the obtained fibrous substrates were examined by a JEOL JSM-5410LV scanning electron microscope (SEM). At least 50 readings of the sizes of the individual fibers and beads from at least five different SEM micrographs were statistically analyzed using SemAphore 4.0 software ($n \geq 50$). The presence of HAp or HAp/proteins in the obtained PCL/PHBV-HAp or PCL/PHBV-HAp/proteins fibrous substrates was also characterized qualitatively by energy dispersive X-ray (EDX) element analysis using the JEOL JSM-5410LV scanning electron microscope (SEM).

Wettability of the obtained fibrous substrates was assessed by water contact angle measurements. The static water contact angles were measured by a sessile drop method using a Krüss contact angle measurement system. A distilled water droplet (10 μL) was randomly placed on the surface of each specimen. At least 10 readings on different positions of the specimen were averaged to attain a data point.

The mechanical integrity, in terms of the tensile strength, Young's modulus, and elongation at break, of the obtained fibrous substrates (rectangular shape, 10 mm × 100 mm) was investigated using a Lloyd LRX universal testing machine (gauge length = 50 mm and crosshead speed = 20 mm·min^{-1}) ($n = 5$).

The true densities of the obtained fibrous substrates ($\rho_{scaffold}$) were measured on ~1 g samples using a Quantachrome Ultrapycnometer-1000 gas pycnometer ($n = 5$). On the basis of the obtained data, the porosities and pore volumes of the matrices can be calculated from the following expressions, respectively: $(1-(\rho_{scaffold}/\rho_{polymer})) \times 100$ and $(1/\rho_{scaffold} - 1/\rho_{polymer})$, where $\rho_{polymer}$

represents the bulk density of the polymeric constituents. Here, $\rho_{PCL/PHBV(50/50\ w/w)}$ was taken as 1.198 $g \cdot cm^{-3}$.

The actual contents of proteins encapsulated in the HAp particles, as well as those of HAp and HAp/proteins particles within the obtained PCL/PHBV-HAp and PCL/PHBV-HAp/proteins composite fibrous substrates were evaluated by a Perkin Elmer TGA7 thermogravimetric analyzer (TGA). The dried sample of HAp or HAp/proteins particles weighing around 5 mg and the fibrous substrate weighing about 20 mg from each sample group were randomly selected. Each specimen was heated from room temperature to 1000°C at a heating rate of 10 °C min^{-1} in air atmosphere.

7.3.6 Release Characteristics of Proteins

The release amounts of the proteins from both HAp/proteins particles and PCL/PHBV-HAp/proteins fibrous substrates were measured by using a bicinchoninic acid (BCA; Pierce Biotechnology, USA) assay. The particles weighing 5 mg or the fibrous substrates (circular discs, ~15 mm in diameter, ~20 mg per disc) were immersed in 1 mL/well of minimum essential medium (MEM; Hyclone, Thermoscientific, USA) of a 24-well tissue-culture polystyrene plate (TCPS; Corning, USA) for various time intervals and then incubated at 37°C. At each time point, 20 μL of the medium was removed and an equally amount of the fresh medium was replaced. The amount of the released proteins in the withdrawn medium was determined by a Thermospectronic Genesis10 UV-visible spectrophotometer at 562 nm. The observed UV absorbance values were converted to the protein concentrations using predetermined standard calibration curves. The measurements were carried out in triplicate.

7.3.7 Cell Culturing

Mouse calvaria-derived, preosteoblastic cells (MC3T3-E1; ATCC CRL-2593) were cultured as monolayers in minimum essential medium with Earle's Balanced Salts (MEM; Hyclone, USA), supplemented by 10% fetal bovine serum (FBS; Biochrom, UK), 1% L-glutamine (Invitrogen, USA), and a 1% antibiotic and antimycotic formulation (containing penicillin G sodium, streptomycin sulfate, and

amphopericin B (Invitrogen, USA)). The medium was changed every other day, and the cultures were maintained at 37 °C in a humidified atmosphere containing 5% CO_2. Each substrate was cut into circular discs (~ 15 mm in diameter), and the disc specimens were placed in wells of a 24-well TCPS (Corning, USA), which was later sterilized in 70% ethanol for 90 min. The specimens were then washed with autoclaved deionized water and subsequently immersed in MEM overnight. To ensure a complete contact between each specimen and the bottom of each well, a metal ring (~12 mm in diameter) was placed on top of the specimen. MC3T3-E1 from the cultures were trypsinized (0.25% trypsin containing 1 mM ethylenediaminetetraacetic acid (EDTA); Invitrogen, USA), counted by a hemacytometer (Hausser Scientific), and seeded at a density of ~40 000 cells cm^{-2} on each of the specimens and the empty wells of a TCPS (i.e., positive control).

For the attachment and proliferation studies, cells were cultured in the same medium as stated previously. For other studies, cells were cultured in MEM supplemented by 2% FBS, 1% L-glutamine, and 1% antibiotic and antimycotic during the first 3 days, after that the cells were cultured in the same medium in the presence of 5 mM glycerol-2-phosphate disodium salt hydrate (β-glycerophosphate; Sigma-Aldrich, USA) and 50 $\mu g \cdot mL^{-1}$ L-ascorbic acid (Sigma-Aldrich, USA).

7.3.8 Cell Attachment and Cell Proliferation

For the attachment study, the cells were allowed to attach to the fibrous substrate specimens and empty wells of a TCPS for 2, 4, and 6 h ($n = 4$). At each time point, the number of the attached cells was quantified by a 3-(4,5-dimethylthiazol-2-yl)-2,5-diphenyl-tetrazolium bromide (MTT; Sigma-Aldrich, USA) assay. For the proliferation study, the cells were first allowed to attach on the specimens and empty wells of a TCPS for 16 h. The number of the proliferated cells was also determined by MTT assay on days 1, 2, and 3 after cell culturing ($n = 4$). The morphology of the cells during the attachment and proliferation periods was observed by SEM.

7.3.9 Quantification of Viable Cells (MTT Assay)

The MTT assay is based on the reduction of the yellow tetrazolium salt to purple formazan crystals by dehydrogenase enzymes secreted from the mitochondria of metabolically active cells. The amount of purple formazan crystals formed is proportional to the number of viable cells. Each cell-cultured specimen was incubated at 37 °C for 30 min with MTT solution, and then a buffer solution containing dimethylsulfoxide (DMSO; Carlo Erba, Italy) (900 μL/well) and glycine buffer (pH = 10) (125 μL/well) was added into each well to dissolve the formazan crystals. Each sample solution was then transferred into a cuvette and placed in a Thermospectronic Genesis10 UV-vis spectrophotometer, from which the absorbance at 570 nm representing the number of viable cells was measured. The observed UV absorbance values were converted to the number of cells using predetermined standard calibration curves.

7.3.10 Morphological Observation of Cultured Cells

After removal of the culture medium, each cell-cultured fibrous scaffold was rinsed with PBS twice, and the cells were then fixed with 3% glutaraldehyde solution (Electron Microscopy Science, USA) at 500 μL/well for 30 min. The specimen was rinsed again with PBS and dehydrated in an ethanol solution of varying concentrations (i.e., 30, 50, 70, 90, and 100%, respectively) for ~2 min at each concentration. It was then dried in 100% hexamethyldisilazane (HMDS; Sigma-Aldrich, USA) for 5 min and later dried in air. The specimens were then observed by SEM, and the morphology of the cells that had been cultured on glass substrates (12 mm in diameter; Menzel, Germany) was used as a positive control.

7.3.11 Alkaline Phosphatase (ALP) Analysis

MC3T3-E1 was cultured on the fibrous substrate specimens and the empty wells of a TCPS for 3 and 7 days to observe the ALP activity ($n = 4$). Each specimen was rinsed with PBS after removal of the culture medium. Alkaline lysis buffer (10 mM Tris-HCl, 2 mM $MgCl_2$, 0.1% Triton-X100, pH 10) (100 μL/well) was added, and the specimen was scrapped and then frozen at –20 °C for ~30 min. An aqueous solution of 2 mg · mL^{-1} *p*-nitrophenyl phosphate (PNPP; Invitrogen,

USA) mixed with 0.1 M aminopropanol (10 μL/well) in 2 mM $MgCl_2$ (100 μL/well) was prepared and added into the specimen, which was then incubated at 37 °C for 30 min. The reaction was stopped by the addition of 0.9 mL/well of 50 mM NaOH, and the extracted solution was measured spectrophotometrically at 410 nm. The amount of ALP was then calculated against a predetermined standard curve and then normalized by the total protein content. In the protein assay, each specimen was treated in the same manner as in the ALP assay up to the point where it was frozen. After freezing, a bicinchoninic acid (BCA; Pierce Biotechnology, USA) solution was added into the specimen and incubated at 37 °C for 30 min. The absorbance of the medium solution was eventually measured at 562 nm by the UV-vis spectrophotometer, and the amount of the total proteins was calculated against a predetermined standard curve.

7.3.12 Mineralization Analysis

Calcium deposition was quantified by Alizarin Red-S (Sigma-Aldrich) staining. MC3T3-E1 had been cultured on the fibrous substrate specimens and the empty wells of a TCPS for 14 days ($n = 4$), after which the cells were fixed with cold methanol for 10 min and washed with deionized water prior to immersion for 3 min in 370 μL of 1% Alizarin Red S (Sigma-Aldrich, USA) solution dissolved in 1:100 (v/v) ammonium hydroxide/water mixture. Each stained specimen was washed several times with deionized water and air-dried at room temperature. The stained specimen was photographed and the redness, signifying the amount of calcium deposition, was quantified by destaining with 10% cetylpyridinium chloride monohydrate (Sigma-Aldrich, USA) in 10 mM sodium phosphate at room temperature for 15 min and spectrophotometrically read at 570 nm.

7.3.13 Statistical Analysis

All values were expressed as mean ± standard deviations. The significance between two data sets was determined by one-way ANOVA analysis using t test for all analyses, except for the attachment, proliferation, and ALP activity analytical studies. Scheffe's test was applied to the three studies. The statistical difference was considered when $p < 0.05$.

7.4 Results and Discussion

7.4.1 Characterization of Fibrous Substrates

The shear viscosity of the polymeric solution is regarded as one of the key parameters affecting the morphology of the electrospun fibrous substrates; this is indicated in Table 7.1 for PCL/PHBV solution as well as PCL/PHBV-HAp and PCL/PHBV-HAp/proteins suspensions. Apparently, the addition of HAp and HAp/proteins particles slightly decreased the shear viscosity of the PCL/PHBV-HAp and PCL/PHBV-HAp/proteins suspension (~400 mPa·s) over that of the PCL/PHBV solution (~431 mPa·s). From the electrospinning process of these solution and suspensions, the fibrous substrates of PCL/PHBV, PCL/PHBV-HAp, and PCL/PHBV-HAp/proteins were fabricated and their surface morphologies are displayed as the representative SEM images in Figure 7.1. The smooth fibers without the presence of the beads were observed in the PCL/PHBV fibrous substrate, while the combination of beaded and smooth fibers was obtained in the PCL/PHBV-HAp and the PCL/PHBV-HAp/proteins composite ones. Hence, the incorporation of the HAp and HAp/proteins particles resulted in the rough fibers. The sizes and densities of the beads were in the range of 3.9–4.7 μm and 4080–4690 beads·mm^{-2} on average, respectively; the sizes of the fibers were in the range of 0.6–0.8 μm on average. The actual sizes of both fibers and beads are also presented in Table 7.1. Evidently, the sizes of the obtained composite fibers decreased with the addition of the particles. The observed decrease in the fiber sizes of the composite fibers in comparison with those of the neat fiber should be the result of the observed decrease in the shear viscosity of the suspensions owing to the existence of the particles. The inclusion of the HAp or HAp/proteins particles in the composite fibrous substrates was qualitatively confirmed by EDX spectra for the element analysis and EDX mapping for the presence of calcium (see Figure 7.2).

All of the fibrous substrates were also characterized for their physico-chemistry in terms of the wettablility using static water contact angle measurements (see Table 7.1). The surface of the PCL/PHBV fibrous substrate appears to be the most hydrophilic, with static water contact angle of 86 ± 4°. The presence of HAp or HAp/proteins particles causes the surface of the composite fibrous substrates to be

slightly more hydrophobic, with the static water contact angles being around 90°. In consistence with the SEM results in Figure 7.1, the observed higher static water contact angle values of the composite fibrous substrates confirmed that the addition of the HAp or HAp/proteins particles resulted in the rougher surface.

Table 7.1 Viscosities of PCL/PHBV solution, PCL/PHBV-HAp and PCL/PHBV-HAp/protein (COL, FN, and CBP) suspensions as well as physical and physico-chemical characteristics of the obtained electrospun fibrous substrates

Sample	Viscosity (mPa·s)	Fiber Diameter (μm)	Bead Size (μm)	Water Contact Angle (deg)
PCL/PHBV	431 ± 6	0.79 ± 0.04	-	86 ± 4
PCL/PHBV-HAp	399 ± 2	0.61 ± 0.15	3.90 ± 0.31	90 ± 1
PCL/PHBV-HAp/COL	392 ± 3	0.66 ± 0.18	3.96 ± 0.79	94 ± 2
PCL/PHBV-HAp/FN	395 ± 4	0.68 ± 0.17	4.61 ± 1.62	92 ± 3
PCL/PHBV-HAp/CBP	401 ± 2	0.60 ± 0.12	4.72 ± 1.49	91 ± 2

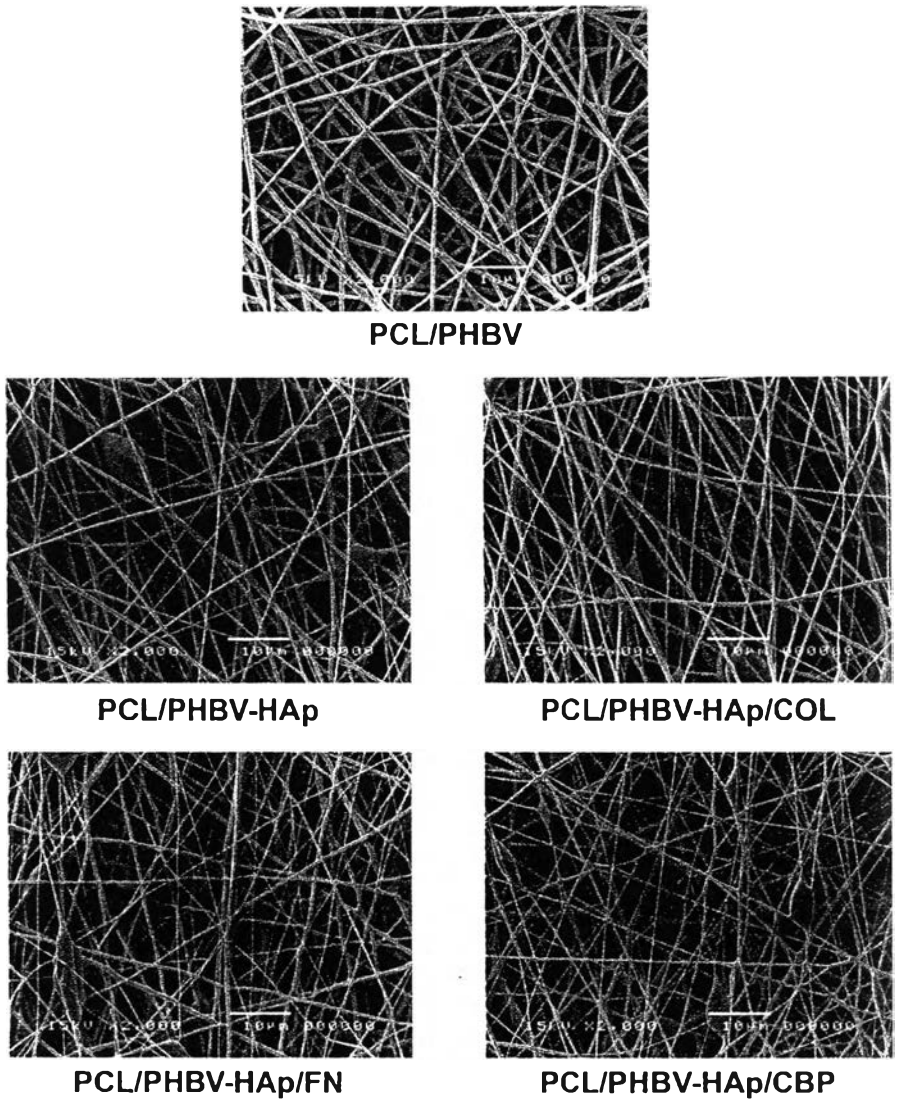

Figure 7.1 Representative SEM images (scale bar = 5 μm and magnification = 2000×) of the electrospun PCL/PHBV fibrous substrate, PCL/PHBV-HAp and PCL/PHBV-HAp/protein (COL, FN, and CBP) composite fibrous substrates.

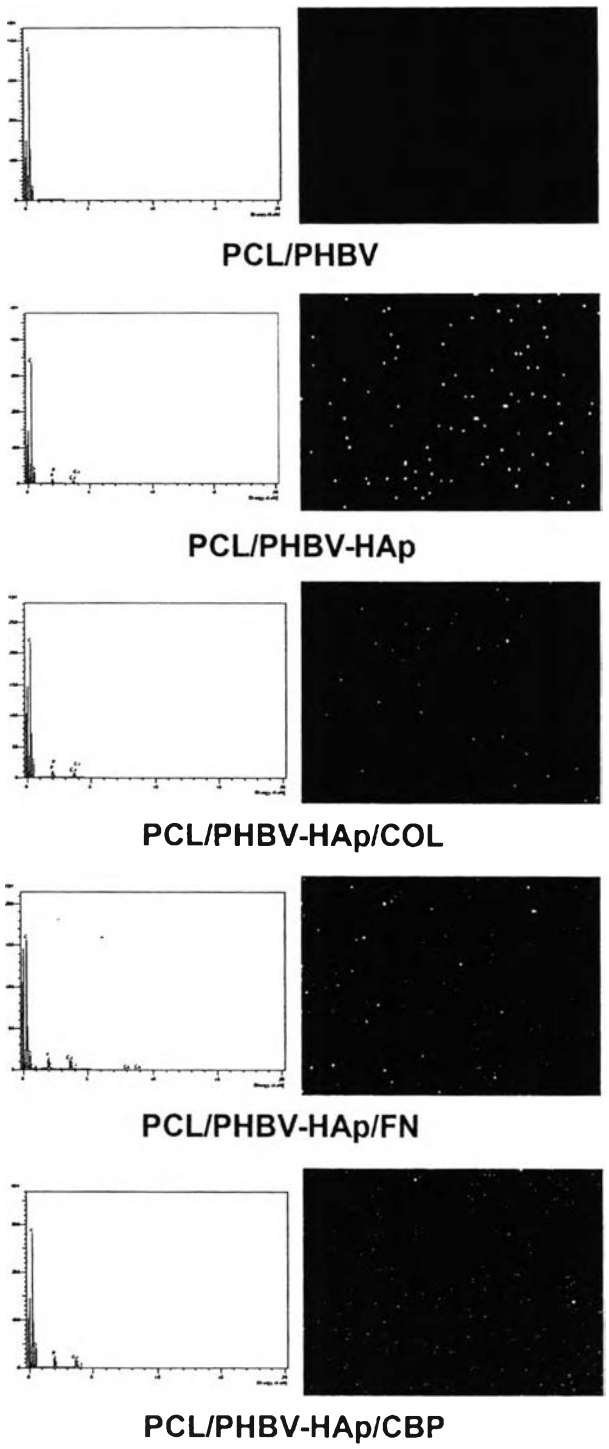

Figure 7.2 Representative EDX images of the element spectra and calcium mappings of the electrospun PCL/PHBV fibrous substrate, PCL/PHBV-HAp and PCL/PHBV-HAp/protein (COL, FN, and CBP) composite fibrous substrates.

The mechanical integrity expressed in terms of the tensile strength, Young's modulus, and elongation at break of the obtained fibrous substrates was evaluated and summarized in Table 7.2. Statistical analysis indicated that the inclusion of the HAp and HAp/proteins in the composite fibrous substrates resulted in a slight decrease in the tensile strength and the elongation at break, from those of the neat fibrous substrate. Nonetheless, the property values of all fibrous substrates were not significantly different. For the Young's modulus, the neat PCL/PHBV fibrous substrate exhibited significantly lower values over all of the composite specimens, which statistically showed equivalent values among themselves. This result agreed well with the report of Chuenjitkuntaworn *et al.* (2010) who found that the presence of HAp obviously improved the compressive rigidity of the scaffolds in an increasing manner with the initial HAp content.

Table 7.2 Mechanical characteristics of the obtained electrospun fibrous substrates

Sample	Tensile Strength (MPa)	Young's Modulus (MPa)	Elongation at Break (%)
PCL/PHBV	1.80 ± 0.13	109.5 ± 1.4	4.7 ± 0.3
PCL/PHBV-HAp	1.73 ± 0.16	128.8 ± 2.4	3.3 ± 0.4
PCL/PHBV-HAp/COL	1.75 ± 0.42	126.4 ± 2.1	3.8 ± 0.6
PCL/PHBV-HAp/FN	1.73 ± 0.18	120.2 ± 3.6	3.2 ± 0.5
PCL/PHBV-HAp/CBP	1.77 ± 0.53	123.7 ± 3.2	4.0 ± 0.5

Table 7.3 shows the true densities, porosities, and pore volumes of all the obtained fibrous substrates. The presence of HAp and HAp/proteins particles increased the true densities and decreased the pore volumes but had no significant effect on the porosities of the composite fibrous substrates. Specifically, the porosity values of all the composite fibrous substrates were about 96% on average, with no specific correlation with the presence of the three types of proteins.

Table 7.3 True densities, porosities, and pore volumes of the obtained electrospun fibrous substrates

Sample	True Density ($\times 10^{-2}$ g·cm^{-3})	Porosity (%)	Pore Volume (cm^3·g^{-1})
PCL/PHBV	3.16 ± 0.35	97.4 ± 0.3	30.8 ± 1.1
PCL/PHBV-HAp	4.02 ± 0.41	96.7 ± 0.5	24.0 ± 1.2
PCL/PHBV-HAp/COL	4.29 ± 0.84	96.4 ± 0.8	22.5 ± 1.0
PCL/PHBV-HAp/FN	4.05 ± 0.39	96.6 ± 0.6	23.9 ± 2.2
PCL/PHBV-HAp/CBP	4.11 ± 0.72	96.6 ± 0.2	23.5 ± 1.8

The thermal degradation of all the obtained specimens was analyzed by TGA to determine the actual contents of the three types of proteins within the HAp particles and those within the PCL/PHBV-HAp/proteins composite fibrous substrates. Figure 7.3 (a) shows TGA thermograms of the HAp incorporating three types of proteins in comparison with the neat HAp. For all of the obtained particles, four stages in the loss of their weight were observed. The first stage (60–200°C) corresponded to the loss of absorbed water, while the second stage (200–400°C) ascribed to the loss of tris-base and proteins from these specimens. The third stage (400–780°C) corresponded to the thermal decomposition of remained organic residues and the final stage (above 780°C) attributed to the loss of carbonate. The char contents at 1000°C in these TGA thermograms could be referred to as the actual amounts of the as-loaded proteins within the HAp particles. The theoretical content of the three kinds of proteins in the protein-loaded HAp particles was 20 wt% (based on the weight of HAp powder). After the thermal experiments from TGA, the actual contents of COL, FN, and CBP within the HAp particles were 10.53, 14.37, and 17.06 wt% (based on the weight of HAp granules), respectively. These values corresponded to around 53, 72, and 85 % (based on the weight of the proteins initially loaded in the HAp granules). The TGA thermograms of the PCL/PHBV, PCL/PHBV-HAp, and PCL/PHBV-HAp/proteins fibrous substrates were also

presented in Figure 7.3 (b). These thermograms showed that the interaction between PCL/PHBV was not interfered by the presence of HAp and HAp/proteins, as the shifts of the curves were not observed. On the basis of this information, the char contents at 980°C in these TGA curves could be referred to as the actual amounts of the as-loaded HAp and HAp/proteins within the PCL/PHBV composite fibrous substrates. The PCL/PHBV fibrous substrates that had been prepared with the initial HAp and HAp/proteins contents of 1% w/v, the actual amounts of HAp, HAp/COL, HAp/FN, and HAp/CBP were determined to be 0.16, 0.20, 0.21, and 0.32% w/v, respectively. The differences between the weight loss of the PCL/PHBV-HAp and the PCL/PHBV-HAp/proteins were calculated to be the actual amounts of COL, FN, and CBP in the PCL/PHBV composite fibrous scaffolds, which were 13, 17, and 51% (based on the weight of the proteins initially loaded in the HAp particles), respectively.

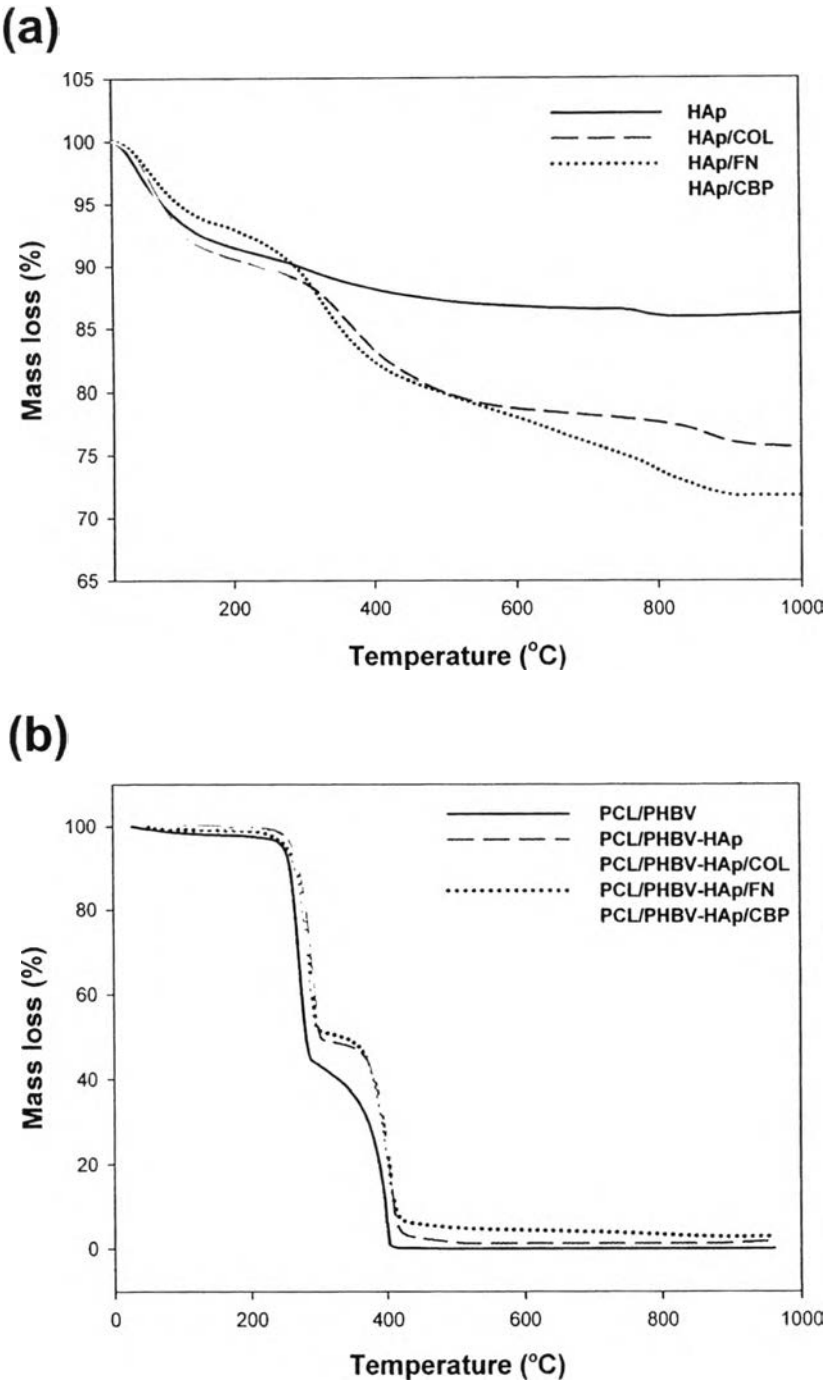

Figure 7.3 TGA thermograms of (a) neat HAp and HAp composite particles and (b) neat PCL/PHBV and PCL/PHBV composite fibrous substrates.

7.4.2 Release Characteristics of Proteins

The release characteristics of the three types of proteins from HAp/proteins composite particles and PCL/PHBV-HAp/proteins composite fibrous substrates were carried out by the BCA assay, using minimum essential medium (MEM) as the transfer medium of a controlled temperature of 37°C. The cumulative amount of the proteins released from the HAp/proteins composite particles and the PCL/PHBV-HAp/proteins composite fibrous substrates as a function of the submersion time is respectively shown in Figure 7.4 (a) and (b). For the release of the proteins from the HAp/proteins particles shown in Figure 7.4 (a), the cumulative amounts of all the proteins increased rather rapidly during the first 7 days with an initial increase in the submersion time. Further increase in the submersion time (from 7 to 14 days) resulted in a gradual increase in the cumulative amounts of all the proteins released to finally assume plateau values at the longest submersion time investigated (i.e., at 28 days). Specifically, at the first day after submersion, the cumulative amount of COL released was the greatest around 13%, followed by those of the FN and CBP released around 6%. Nonetheless, the opposite results of the cumulative amounts of these three proteins released were observed after 1 day. The released values of CBP, FN, and COL eventually increased to about 75, 64, and 42% after the HAp/proteins composite particles had been submerged in the medium for 28 days, respectively. At the same period of time, a slightly different behavior of the proteins released from PCL/PHBV-HAp/proteins composite fibrous substrates was observed (see Figure 7.4 (b)). The cumulative amounts of all types of proteins released from the PCL/PHBV-HAp/proteins composite fibrous substrates occurred slowly during the first 4 days after submersion in the releasing medium. Interestingly, the cumulative amounts of CBP and FN released increased rather rapidly from 4 to 14 days, and reached the plateau values about 36 and 30% at day 28, respectively, while that of COL released increased gradually from 4 to 10 days, and finally became a plateau values about 18% at day 28.

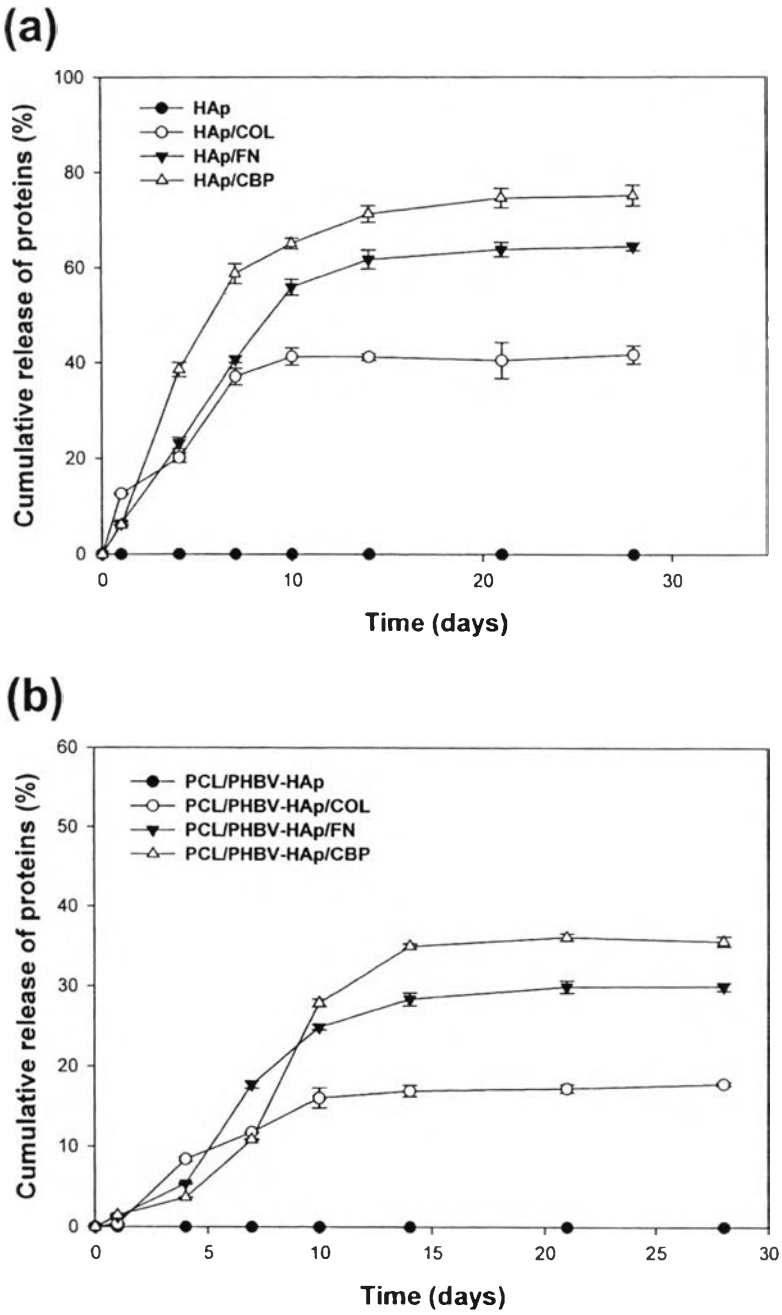

Figure 7.4 Cumulative release of proteins from (a) HAp composite particles and (b) PCL/PHBV composite fibrous substrates, in terms of the percentage of the weight of the proteins released divided by the actual weight of the proteins in the specimens, as a function of submersion time in MEM, at 37 °C ($n = 3$).

7.4.3 Cell Attachment and Cell Proliferation

The potential for all types of fibrous substrates in supporting both the attachment and the proliferation of bone cells was assessed with MC3T3-E1. Figure 7.5 shows the quantitative analysis of the numbers of cells attached after cell seeding on the surfaces of all types of fibrous substrates and TCPS for 2, 4, and 6 h. At 2 and 4 h, the number of cells attached on the surface of the neat PCL/PHBV fibrous substrate is similar to that on the surface of TCPS, whereas those of the cells attached on the surfaces of the other composite fibrous substrates seemed to be inferior to that on the surface of TCPS. At 6 h, the number of cells attached on the surface of PCL/PHBV-HAp/COL was slightly higher than those on the surfaces of the other fibrous substrates; however, the attachment of the cells on the surfaces of all types of fibrous substrates were still lower than that on the surface of TCPS.

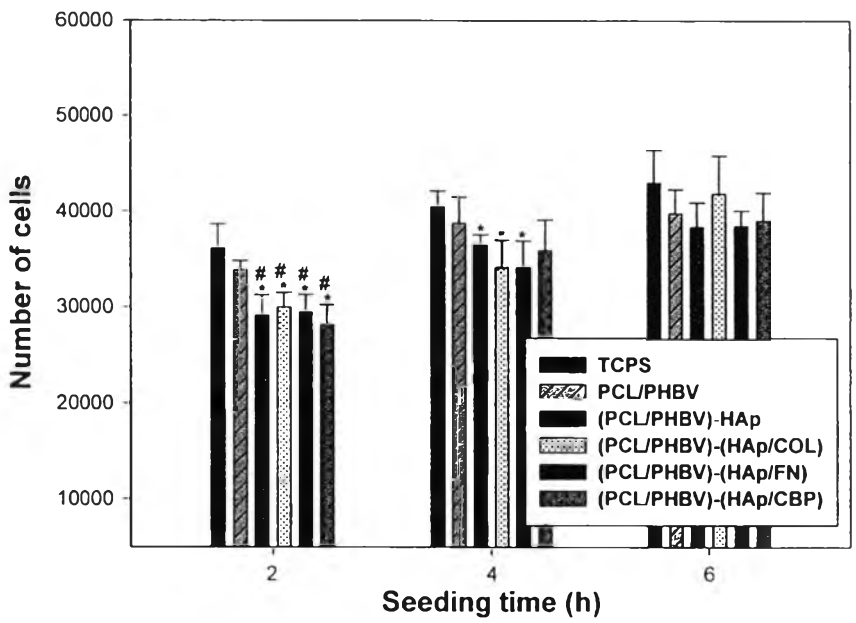

Figure 7.5 Attachment of MC3T3-E1 that were seeded onto the surfaces of TCPS and various types of fibrous substrates as a function of the cell seeding time. *Significance at $p < 0.05$ with respect to TCPS. #Significance at $p < 0.05$ with respect to the fibrous substrate from PCL/PHBV solution.

Figure 7.6 (a) shows the quantitative analysis of the proliferation of MC3T3-E1 after cultured on the surfaces of all types of fibrous substrates and TCPS for 1–3 days. On days 1 and 2, the numbers of the cells on the surface of three types of PCL/PHBV-HAp/proteins fibrous substrates were slightly greater than those on the surfaces of PCL/PHBV-HAp and neat PCL/PHBV fibrous substrates. In comparison with that on TCPS, the proliferation of the cells on all types or fibrous substrates was still lower. The lesser number of cells in the proliferation period on all types of the fibrous substrates in comparison to that on TCPS could be owing to the lesser number of cells that were able to attach on the rough and less hydrophilic surface of the fibrous substrates in comparison to the smoother and more hydrophilic surface of TCPS (Wutticharеonmongkol *et al.*, 2007). On day 3, the number of cells on the surface of PCL/PHBV-HAp/CBP fibrous substrate exhibited the greatest value, followed by those on the surfaces of PCL/PHBV-HAp/FN, PCL/PHBV-HAp/COL, PCL/PHBV-HAp, and neat PCL/PHBV fibrous substrates, respectively. The number of cells on the surface of the neat PCL/PHBV fibrous substrates was equivalent to that on the surface of TCPS. Apparently, despite the lower number of attached cells, the fibrous substrates could support the proliferation of MC3T3-E1 at similar levels to that of the cells on TCPS, with the cells grown on PCL/PHBV-HAp/CBP showing the greatest proliferation rate on day 3.

In the attempt to investigate the effects of proteins released to the proliferated cells, the quantitative analysis of the proliferation of MC3T3-E1 after having been cultured on the surfaces of TCPS with and without the presence of HAp or HAp/proteins particles is displayed in Figure 7.6 (b). Interestingly, on days 1 and 2, the numbers of the cells on the surfaces of TCPS with the presence of HAp/COL showed the highest values, followed by those on the surfaces of TCPS with the presence of HAP/FN, HAp/CBP, and HAp, and that on the surface of the neat TCPS, respectively. On day 3, the number of the cells on the surface of the TCPS with the presence of the HAp/CBP composite particle appeared to be the greatest value, followed by those of the TCPS with HAp/FN, HAp/COL, and HAp, and that on the surface of the neat TCPS, respectively. These results were consistent with the release characteristics of the three types of proteins in Figure 7.4 (a), confirming the influence of the proteins released on the cell growth. Therefore, the presence of

HAp/proteins particles within the PCL/PHBV fibrous substrates could help regulate the proliferation of the cells.

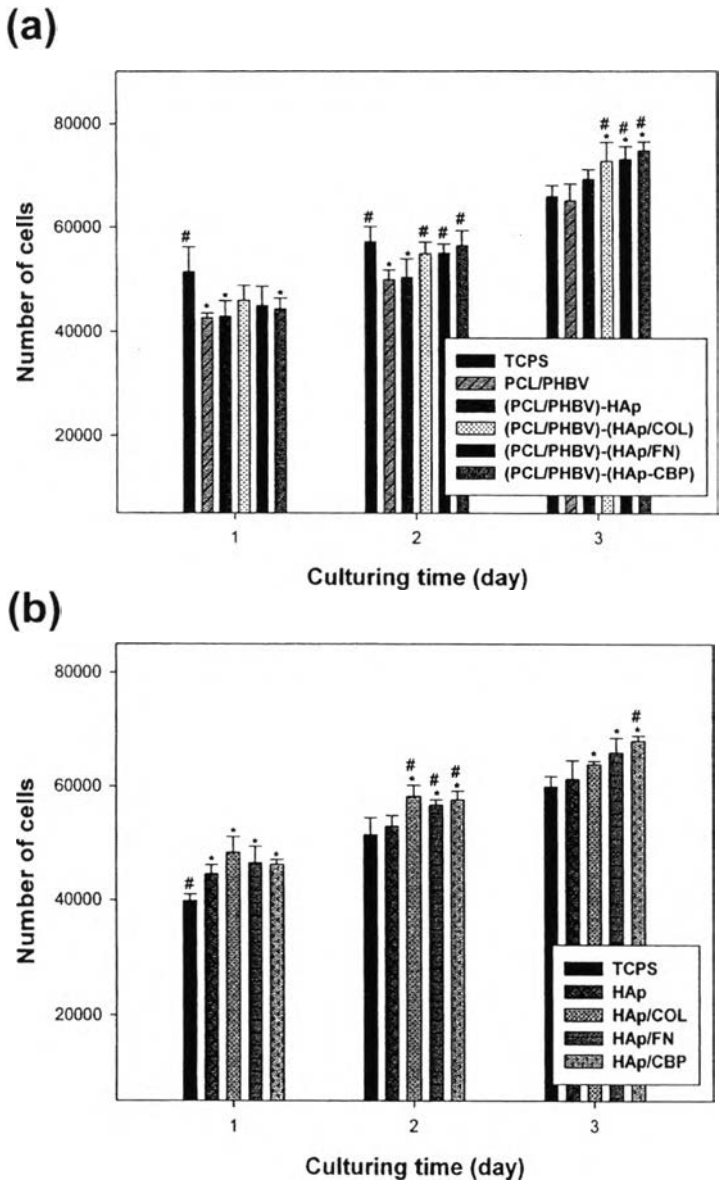

Figure 7.6 Proliferation of MC3T3-E1 that were cultured on the surfaces of (a) TCPS and various types of fibrous substrates and (b) TCPS without and with HAp and HAp/proteins particles as a function of the cell culturing time. *Significance at $p < 0.05$ with respect to TCPS. #Significance at $p < 0.05$ with respect to (a) the fibrous substrate from PCL/PHBV solution and (b) TCPS with HAp particle.

Figure 7.7 shows selected SEM images of MC3T3-E1 that had been cultured on the surfaces of glass and all types of fibrous substrates for various time intervals. At 2 h after cell seeding, the majority of the cells on virtually all types of substrates were still round, expect for those on the surfaces of PCL/PHBV-HAp/CBP, PCL/PHBV-HAp/FN, and PCL/PHBV-HAp/COL solutions that revealed an evidence of filopodia. At 4 and 6 h after cell seeding, the majority of the cells began to expand their cytoplasm over the surfaces of all types of substrates. On days 1 and 2 after cell culturing, the cells proliferated to cover ~50 to ~60% of the surfaces on almost all types of fibrous substrates, except for those on the surfaces of the fibrous substrates from PCL/PHBV-HAp/FN and PCL/PHBV-HAp/COL solutions that exhibited the cell proliferated to cover ~70% of the surfaces. On day 3, full expansions of the cells on all types of substrates were observed. Evidently, most of the cell expansions were noticed for the cells on the surfaces of the fibrous substrates from PCL/PHBV-HAp/CBP solution, which proliferated to cover ~80% of the surface. On the basis of the results demonstrated in Figure 7.7, the fibrous substrate from PCL/PHBV-HAp/CBP solution appeared to be the best among the examined fibrous substrates for supporting the growth of MC3T3-E1. The best support of the PCL/PHBV-HAp/CBP fibrous substrate for bone cell culture could be due to the presence of HAp and CBP, which have osteoconductive and osteoinductive properties, respectively.

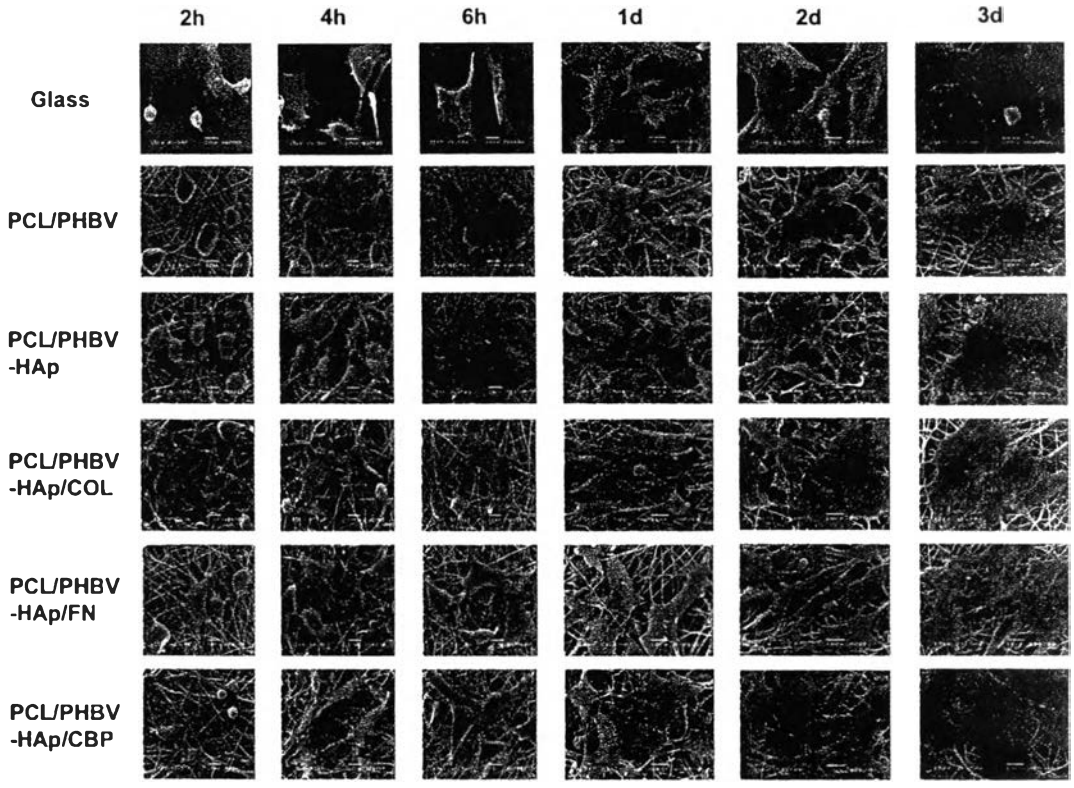

Figure 7.7 Representative SEM images (scale bar = 10 μm and magnification = 1500×) of MC3T3-E1 that were seeded/cultured on the surfaces of a glass substrate (control) and various types of fibrous substrates at various time points.

7.4.4 Alkaline Phosphatase (ALP) Activity

The ALP activity of MC3T3-E1 that had been cultured on TCPS and all types of fibrous substrates was monitored on days 3 and 7 after cell culturing (see Figure 7.8 (a)). On day 3, The ALP activities of the cells that had been grown on the surfaces of the fibrous substrates from PCL/PHBV-HAp/CBP, PCL/PHBV-HAp/FN, and PCL/PHBV-HAp/COL solutions were not statistically different; however, they were greater than those of the cells on the rest of the fibrous substrates and TCPS. The ALP activity from that observed on day 3 of the cells that had been grown on all types of substrates obviously increased with a further increase in the time in culture on day 7. The cells that had been grown on the surfaces of the fibrous substrates from PCL/PHBV-HAp/CBP, PCL/PHBV-HAp/FN, and PCL/PHBV-HAp/COL solutions displayed higher levels of ALP activity that are statistically equivalent to those that

had been grown on TCPS, while the cells that had been grown on the surfaces of other types of fibrous substrates had significantly lower values. These results should be owing to the expression of sufficient amounts of CBP, FN, and COL, which can trigger the secretion of ALP (Choi *et al.*, 1996). The fibrous substrates from both PCL/PHBV-HAp/CBP and PCL/PHBV-HAp/FN solutions could enhance the ALP production of MC3T3-E1 much better than the rest of other types of fibrous substrates. However, the fibrous substrate from PCL/PHBV-HAp/CBP solution could promote the ALP production of the cells slightly better than that from PCL/PHBV-HAp/FN solution.

The effects of the three types of proteins released on the secretion of ALP from MC3T3-E1 that had been cultured on TCPS with and without the presence of HAp and HAp/proteins particles for 3 and 7 days were also investigated (see Figure 7.8 (b)). On day 3, the ALP activities of the cells that had been grown on the surfaces of TCPS with and without the presence of HAp/protein particles were statistically the same, which appeared to be greater than that of the cells on the surface of TCPS with the presence of HAp. On day 7, substantial increases in the ALP activity from that noticed on day 3 of the cells that had been grown on all types of substrates were clearly seen. The cells that had been grown on the surfaces of TCPS with the presence of HAp/CBP, HAp/FN, and HAp/COL exhibited significantly higher levels of ALP activity than those on the surfaces of TCPS with HAp and the neat TCPS. Apparently, the TCPS with the presence of HAp/CBP was able to enhance the ALP production of MC3T3-E1 much better than other types of substrates. These results corroborated that the three types of proteins released could support the expression of ALP from MC3T3-E1.

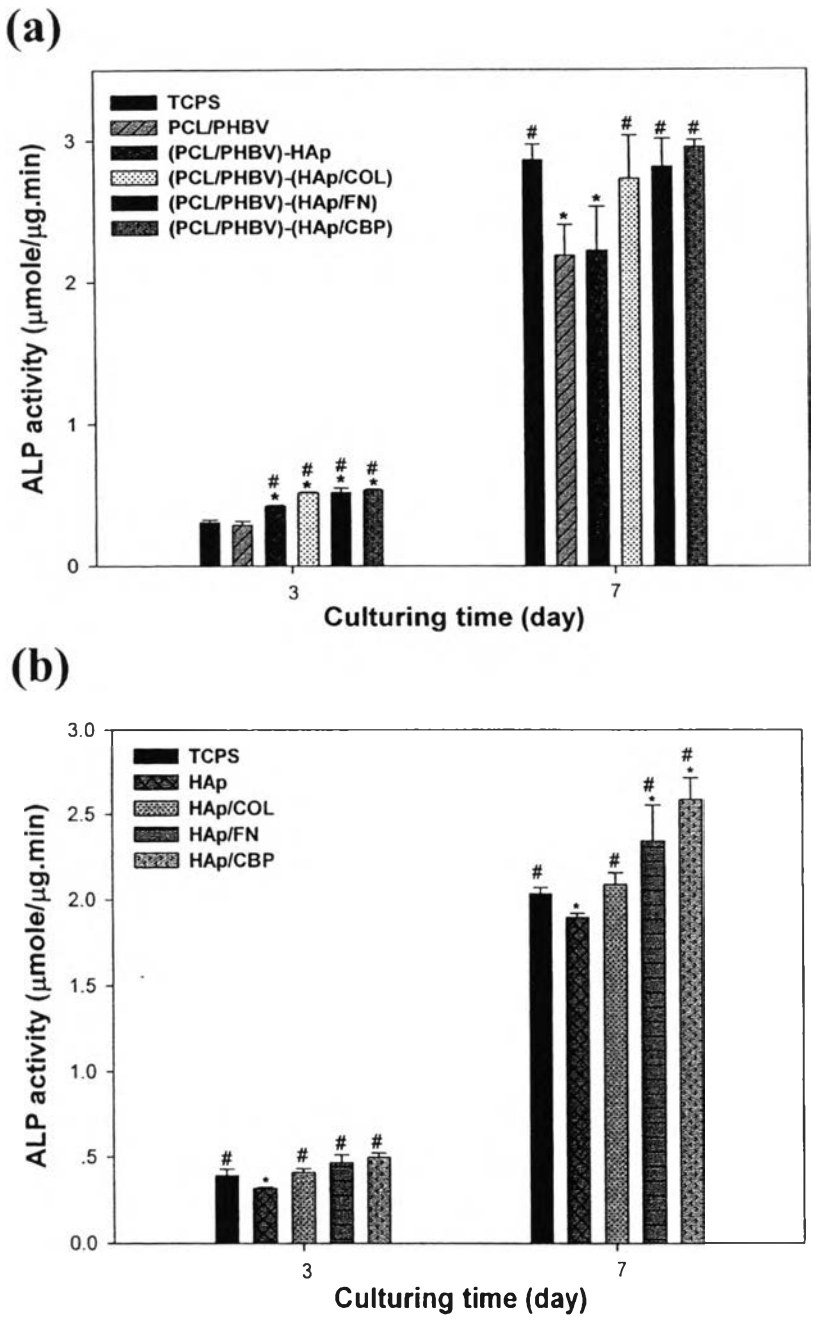

Figure 7.8 ALP activity of MC3T3-E1 that was cultured on the surfaces of (a) TCPS and various types of fibrous substrates and (b) TCPS without and with HAp and HAp/proteins particles at various given time points after cell culturing. *Significance at $p < 0.05$ with respect to TCPS. #Significance at $p < 0.05$ with respect to (a) the fibrous substrate from PCL/PHBV solution and (b) TCPS with HAp particle.

7.4.5 Mineralization

Photographic images of Alizarin Red S staining of MC3T3-E1 that had been cultured on TCPS and all types of fibrous substrates for 14 days, together with their quantitative analyses, are shown in Figure 7.9 (a) and (b), respectively. In the presence of calcium, the staining product (i.e., an Alizarin Red S-calcium chelating product) appeared red. The cells that had been cultured on all types of the fibrous substrates stained positively for calcium deposition. Remarkably, the cells that had been cultured on the fibrous substrates from PCL/PHBV-HAp/CBP solution demonstrated the greatest intensity, followed by those that had been cultured on the fibrous substrates from PCL/PHBV-HAp/FN, PCL/PHBV-HAp/COL, PCL/PHBV-HAp, PCL/PHBV solutions, respectively. Hence, the incorporation of protein-loaded HAp particles into the PCL/PHBV fibrous substrates appeared to considerably enhance not merely the ALP activity, but the mineralized extracellular matrix of MC3T3-E1 as well.

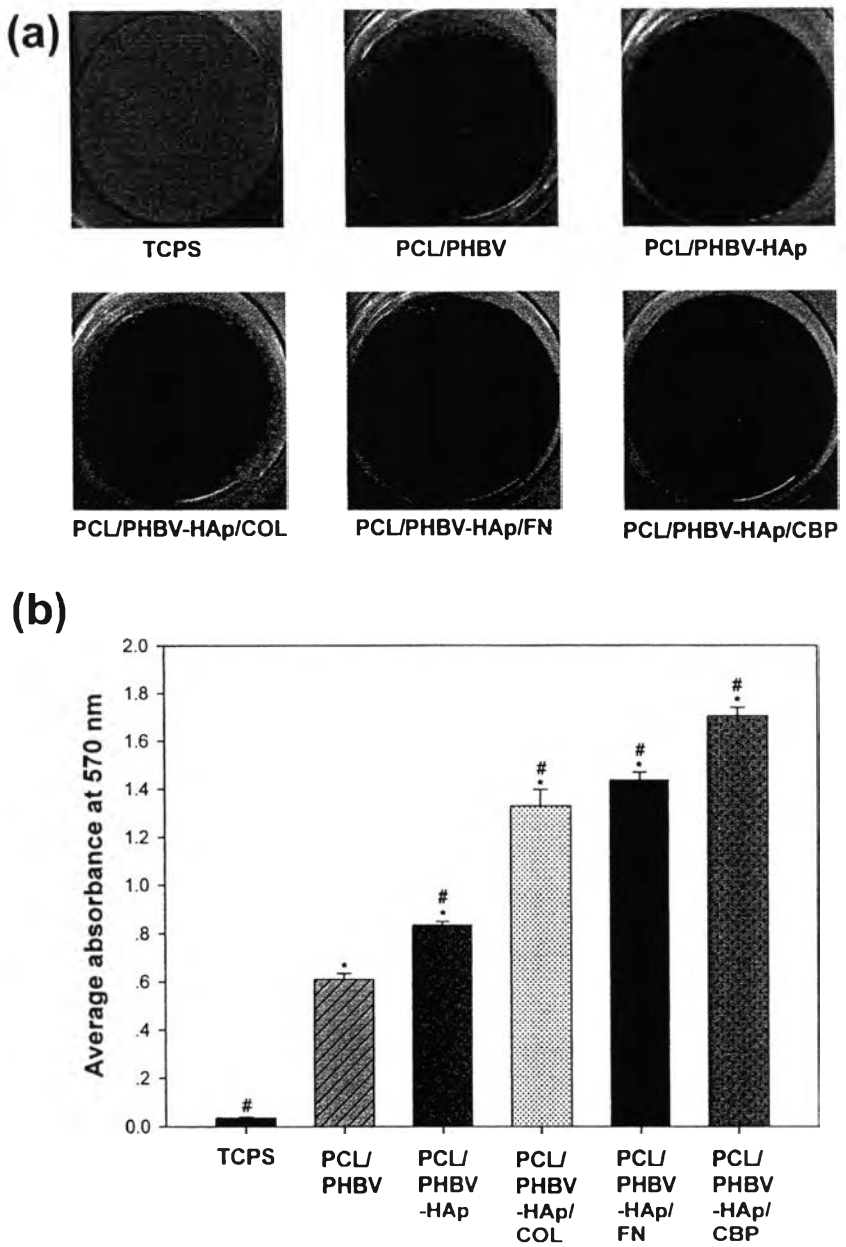

Figure 7.9 Alizarin Red S staining for the mineralization of MC3T3-E1 on day 14 after being cultured on the surfaces of TCPS and various types of the fibrous substrates: (a) photographic images of the stained specimens and (b) the corresponding quantitative analyses. *Significance at $p < 0.05$ with respect to TCPS. #Significance at $p < 0.05$ with respect to the fibrous substrate from PCL/PHBV solution.

7.5 Conclusions

Electrospinning was used to fabricate fibrous substrates of PCL/PHBV with and without the presence of neat HAp and HAp loaded with COL, FN, and CBP (HAp/proteins) particles. The amount of HAp and HAp/proteins particles in the composite fibrous substrates was 1% (w/v, based on the volume of the based PCL/PHBV solution, i.e. 10 wt % in 80/20 v/v chloroform/DMF). The existence of all types of HAp particles made the morphologies of the individual fibers slightly less uniform and rougher, resulting in slightly more hydrophobic surfaces of the composite fibrous substrates. The release characteristics of the three types of proteins from HAp/proteins composite particles occurred rather rapidly during the first 7 days and increased gradually afterward, while those from PCL/PHBV-HAp/proteins composite fibrous substrates occurred gradually over the testing period. The cumulative amount of CBP released was the greatest from both HAp/CBP composite particle around 75% and PCL/PHBV-HAp/CBP composite fibrous substrate around 36%. All types of fibrous substrates as bone-scaffolding materials were further evaluated with MC3T3-E1 mouse pre-osteoblastic cells. The results demonstrated that the PCL/PHBV-HAp/CBP was the best to support the proliferation, differentiation, and mineralization of the cells. Along with the greatest intensity of calcium deposits observed for the cells grown on the PCL/PHBV-HAp/CBP composite fibrous substrate for 14 days, the presence of HAp and CPB in the PCL/PHBV-HAp/CBP composite fibrous substrates certainly enhanced both osteoconductivity and osteoinductivity of the materials.

7.6 Acknowledgments

The authors acknowledge the partial support received from 1) The Thailand Research Fund (TRF, grant no.: DBG5280015), 2) The Institute for the Promotion of Teaching Science and Technology (IPST, for the doctoral scholarship of P.K.), 3) The Petroleum and Petrochemical College (PPC), Chulalongkorn University, and 4) Center of Excellence on Petrochemical and Materials Technology (PETRO-MAT), Chulalongkorn University.

7.7 References

Akao, M., Sakatsume, M., Aoki, H., Takagi, T., and Sasaki, S. (1993) In-vitro mineralization in bovine tooth germ-cell cultured with sintered hydroxyapatite. Journal of Materials Science: Materials in Medicine, 4, 569-574.

Boland, E.D., Pawlowski, K.J., Barnes, C.P., Simpson, D.G., Wnek, G.E., and Bowlin G.L. (2006) Electrospinning of bioresorbable polymers for tissue engineering scaffolds. ACS Symposium Series: Polymeric Nanofiber, 918, 188-204.

Chew, S.Y., Wen, J., Yim, E.K.F., and Leong, K.W. (2005) Sustained release of proteins from electrospun biodegradable fibers. Biomacromolecules, 6, 2017-2024.

Choi, J.Y., Lee, B.H., Song, K.B., Park, R.W., Kim, I.S., Sohn, K.Y., Jo, J.S., and Ryoo, H.M. (1996) Expression patterns of bone-rated proteins during osteoblastic differentiation in MC3T3-E1. Journal of Cellular Biochemistry, 61, 609-618.

Chuenjitkuntaworn, B., Inrung, W., Damrongsri, D., Mekaapiruk, K., Supaphol, P., and Pavasant, P. (2010) Polycaprolactone/hydroxyapatite composite scaffolds: preparation, characterization, and *in vitro* and *in vivo* biological responses of human primary bone cells. Journal of Biomedical Materials Research Part A, 94, 241-251.

Del, G.C., Ercolani, E., Nanni, F., and Bianco, A. (2011) Assessment of Poly(ε-caprolactone)/poly(3-hydroxybutyrate-*co*-3-hydroxyvalerate) (PCL/PHBV) blends processed by solvent casting and electrospinning. Materials Science and Engineering: A, 528, 1764-1772.

Deng, X.L., Xu, M.M., Li, D., Sui, G., Hu, X.Y., and Yang X.P. (2007) Electrospun PLLA/MWNTs/HA Hybrid Nanofiber Scaffolds and Their Potential in Dental Tissue Engineering. Key Engineering Materials, 330, 393-396.

Gonçalves, S.P.C. and Martins-Franchetti, S.M. (2011) Action of soil microorganisms on PCL and PHBV blend and films. Journal of Polymers and Environment, 18, 714-719.

Hench, L.L. and Polak, J.M. (2002) Third-generation biomedical materials. Science, 295, 1009-1014.

Hubbell, J.A. (1995) Biomaterials in tissue engineering. Bio/Technology, 13, 365-376.

Hutmacher, D.W. (2000) Scaffolds in tissue engineering bone and cartilage. Biomaterials, 2, 2529-2543.

Ito, Y. (1998) Tissue engineering by immobilized growth factors. Materials Science and Engineering: C, 6, 267-274.

Kenawy, E.R., Abdel-Hay, F.I., El-Newehy, M.H., and Wnek, G.E. (2009) Processing of polymer nanofibers through electrospinning as drug delivery system. Materials Chemistry and Physics, 113, 296-302.

K-hasuwan, P., Pavasant, P., and Supaphol, P. (2011) Effect of the surface topography of electrospun poly(ε-caprolactone)/poly(3-hydroxybyterate-co-3-hydroxyvalerate) fibrous substrates on cultured bone cell behavior. Langmuir, 27, 10938-10946.

Luklinska, Z.B. and Schluckwerder, H. (2003) *In vivo* response to HA-polyhydroxybutyrate/polyhydroxyvalerate composite. Journal of Microscopy, 211, 121-129.

Ndreu, A., Nikkola, L., Ylikauppila, H., Ashammakhi, N., and Hasirci, V. (2008) Electrospun biodegradable nanofibrous mats for tissue engineering. Nanomedicine, 3, 45-60.

Prabhakaran, M.P., Venugopal, J., and Ramakrishna, S. (2009) Electrospun nanostructured scaffolds for bone tissue engineering. Acta Biomaterialia, 5, 2884-2893.

Rameshbabu, N., Rao, K.P., and Kumar T.S.S. (2005) Accelerated microwave processing of nanocrystalline hydroxyapatite. Journal of Materials Science, 40, 6319-6323.

Sangsanoh, P., Waleetorncheepsawat, S., Suwantong, O., Wutticharoenmongkol, P., Weeranantanapan, O., Chuenjitbuntaworn, B., Cheepsunthorn, P., Pavasant, P., and Supaphol, P. (2007) In vitro biocompatibility of Schwann cells on surfaces of biocompatible polymeric electrospun fibrous and solution-cast film scaffolds. Biomacromolecules, 8, 1587-1594.

Vaquette, C., Kahn, C., Frochot, C., Nouvel, C., Six, J.L., De Isla, N., Luo, L.H., Cooper-White, J., Rahouadj, R., and Wang, X. (2010) Aligned poly(L-lactic-*co*-e-caprolactone) electrospun microfibers and knitted structure: A novel composite scaffold for ligament tissue engineering. Journal of Biomedical Materials Research Part A, 94, 1270-1282.

Venugopal, J., Vadgama, P., Sampath Kumar, T.S., and Ramakrishna, S. (2007) Biocomposite nanofibers and osteoblasts for bone tissue engineering. Nanotechnology, 18, 1-8.

Wutticharеonmongkol, P., Pavasant, P., and Supaphol, P. (2007) Osteoblastic phenotype expression of MC3T3-E1 cultured on electrospun polycaprolactone fiber mats filled with hydroxyapatite nanoparticles. Biomacromolecules, 8, 2602-2610.

Yuan, H.Z., Yang, Z., Li, Y., and Zhang, X. (1998) Osteoinduction by calcium phosphate biomaterials. Journal of Materials Science: Materials in Medicine, 9, 723-726.